

Quantum optical coherence can survive photon losses using a continuous-variable quantum erasure-correcting code

Mikael Lassen^{1,2*}, Metin Sabuncu^{1,2}, Alexander Huck¹, Julien Niset^{3,4}, Gerd Leuchs^{2,5}, Nicolas J. Cerf³ and Ulrik L. Andersen^{1*}

A fundamental requirement for enabling fault-tolerant quantum information processing is an efficient quantum error-correcting code that robustly protects the involved fragile quantum states from their environment^{1–10}. Just as classical error-correcting codes are indispensable in today's information technologies, it is believed that quantum error-correcting code will play a similarly crucial role in tomorrow's quantum information systems. Here, we report on the experimental demonstration of a quantum erasure-correcting code that overcomes the devastating effect of photon losses. Our quantum code is based on linear optics, and it protects a four-mode entangled mesoscopic state of light against erasures. We investigate two approaches for circumventing in-line losses, and demonstrate that both approaches exhibit transmission fidelities beyond what is possible by classical means. Because in-line attenuation is generally the strongest limitation to quantum communication, such an erasure-correcting code provides a new tool for establishing quantum optical coherence over longer distances.

Quantum information protocols are inevitably affected by noise, which in turn produces errors in the extremely sensitive processed quantum information¹. To take full advantage of quantum information processing, including long-distance quantum communication and fault-tolerant quantum computing^{11–13}, these errors must be corrected efficiently. This can be done by encoding the information in special quantum error-correcting codes, which introduce redundancy, protecting the fragile quantum information from environment-induced decoherence. Using such codes, transmission errors can be diagnosed through so-called syndrome measurements, the results of which are used to correct the corrupted quantum information.

Quantum error correcting codes (QECC) were first discovered for discrete variable qubit systems^{2–7} and later extended to systems in which information is encoded into observables with a continuous spectrum^{8–10,14,15}. Only a few experimental implementations demonstrating quantum error correction have been carried out to date, such as those in nuclear magnetic resonance systems¹⁶, in an ion-trap system¹⁷, and in a pure optical system^{18,19}. All these works have reported on the correction of errors that are the manifestation of line noise. However, it is very often the loss of photons in a transmission line (corresponding to erasures in an information theoretic language) that is the main obstacle to the survival of quantum coherence. Here, we report on the first experimental realization of a quantum erasure-correcting code that

simultaneously protects two independent continuous-variable (CV) quantum systems against photon losses in the transmission channel.

We consider the transmission of a quantum state of light through a channel that either transmits the information perfectly or completely erases it with an error probability P_E . The density matrix of the transmitted state is given by

$$\rho = (1 - P_E)|\alpha\rangle\langle\alpha| + P_E|0\rangle\langle 0| \quad (1)$$

where the state $|\alpha\rangle$ comprises the transmitted quantum information and $|0\rangle$ is the vacuum state arising due to channel erasure. Such an error model, which can be viewed as random fading, is likely to occur as a result of time jitter noise or beam pointing noise in an atmospheric transmission channel, for example^{20–22}. The CV code for protecting quantum information from erasures is a four-mode entangled mesoscopic state in which two (information-carrying) quantum states are encoded with the help of a two-mode entangled vacuum state¹⁵. As a result of the redundancy, the damage that the erasure has made regarding the quantum states can be reversed by a simple decoding procedure followed by measurements that determine the damage and a feedforward step that corrects the output states. It is remarkable that the quantum coding, decoding and correction is based on simple linear optical components and Gaussian resources. This is not a violation of the recent No-Go theorem for QECC of Gaussian states with Gaussian transformation²³ because the stochastic erasure noise occurring in the transmission channel produces a non-Gaussian state.

We investigate two different detection strategies for correcting the corrupted quantum states. The first strategy actively corrects the errors of the transmitted state according to the outcome of the measurement, whereas the second strategy filters out the corrupted state when an error is detected. A fundamental difference between the two approaches is that the former is deterministic and therefore always recovers a corrected output state, whereas the latter is probabilistic, which means that the corrected output state is only sometimes recovered. As for most QECC schemes, the deterministic approach comes with a price: for the scheme to work one may only allow for the occurrence of a given number of errors (a single error in this case) and one needs to know in which mode the error occurred after the transmission of the particular quantum state. As was shown in ref. 15, these requirements may, however, be relaxed by using a probabilistic approach. We note

¹Department of Physics, Technical University of Denmark, Fysikvej, 2800 Kongens Lyngby, Denmark, ²Max Planck Institute for the Science of Light, Günther Scharowskystrasse 1, 91058 Erlangen, Germany, ³Quantum Information and Communication, Ecole Polytechnique, CP 165, Université Libre de Bruxelles, 1050 Brussels, Belgium, ⁴Department of Physics, Hunter College of CUNY, 695 Park Avenue, New York, New York 10065, USA, ⁵University Erlangen-Nürnberg, Staudtstrasse 7/B2, 91058 Erlangen, Germany. *e-mail: mlassen@fysik.dtu.dk; ulrik.andersen@fysik.dtu.dk

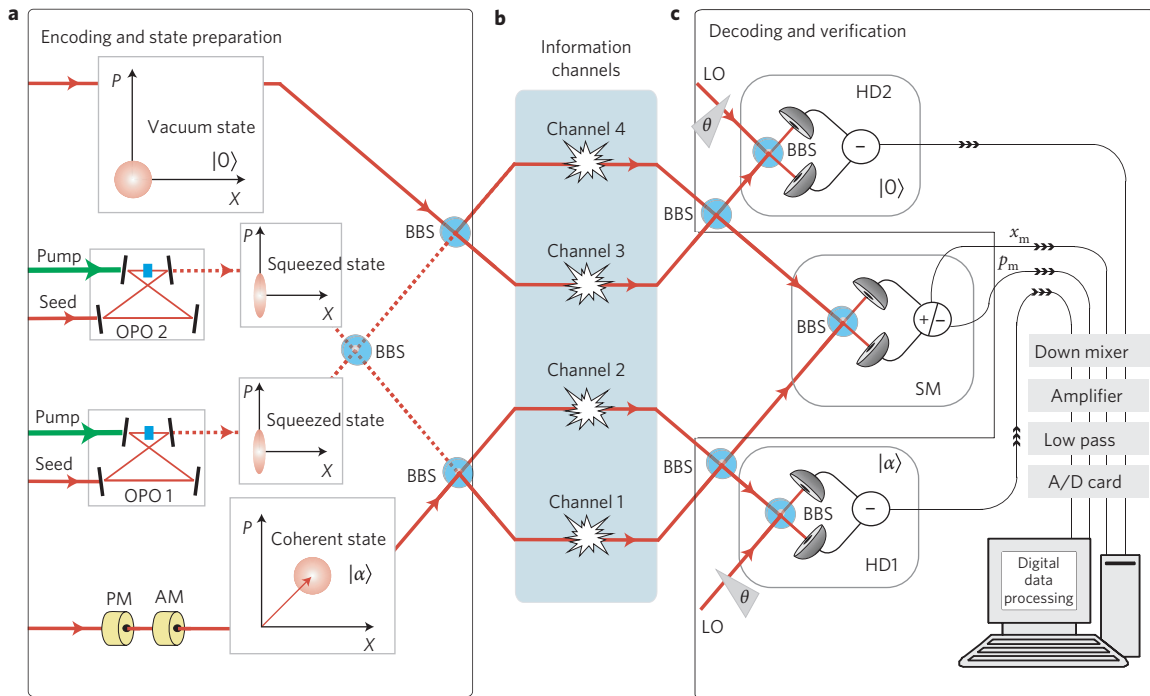


Figure 1 | Schematics of the experimental QECC set-up. **a**, The four-mode code is prepared through linear interference at three balanced beamsplitters (BBS) between the two input states, $|\alpha\rangle$ and $|0\rangle$, and two ancillary squeezed vacuum states. The latter states are produced in two optical parametric oscillators, OPO 1 and OPO 2, and the coherent state is prepared via a coherent modulation at 5.5 MHz produced by an amplitude (AM) and a phase modulator (PM). **b**, The encoded state is injected into four free-space channels that can be independently blocked, thereby mimicking erasures. **c**, The corrupted state is decoded, the error is detected by the syndrome measurement (SM) and the state is deterministically corrected or probabilistically selected. The measurement is an entangled measurement in which the phase and amplitude quadratures of the two emerging states are jointly measured (for example, see ref. 25). The error correcting displacement or post-selection operation is carried out electronically after the measurement of the transmitted quantum states. These states are measured with two independent homodyne detectors that allow for full quantum state characterization, by scanning the phases (θ) of the local oscillators (LOs) with respect to the phases of the signals. All erasure events are obtained by blocking the beam paths.

that a subpart of the deterministic circuit has been implemented in the context of CV quantum secret sharing²⁴.

Schematics of the set-up are depicted in Fig. 1, showing an encoding station where the four-mode code is prepared, an erasure channel where information is randomly erased, and a decoding station, where measurement outcomes either correct or filter the corrupted state. The key element in the preparation stage is a two-mode Gaussian entangled source, which exhibits quantum correlations between pairs of conjugate quadrature amplitudes (see Methods). This state interferes with two signal states to form the final four-mode code comprising four optical beams. A vacuum state is chosen as one of the input signals, and the other input is prepared in a coherent state. This choice simplifies the experimental realization, but is not an intrinsic limitation of the scheme. The four resulting beams are then dispersed into four free-space transmission channels that can be independently blocked to simulate any combination of erasures. At the decoding station the interferences are reversed in two balanced beamsplitters, and two of the resulting outputs are jointly measured in an entangled measurement strategy²⁵ in which the modes interfere on a balanced beamsplitter and conjugate quadratures are measured at the two outputs (see Fig. 1). The resulting outcomes are now used either to deterministically correct the errors through conditional linear displacements or to probabilistically filter out the loss-infected states.

First, we describe the deterministic correction strategy. Figure 2a shows a scan of the quantum-mechanical oscillator comprising the coherent state quantum information of the input state. The information encoded in a coherent state can be concisely described by the conjugate quadrature operators: the amplitude \hat{x} and the phase \hat{p} such that $|\alpha\rangle = |\langle\hat{x}\rangle + i\langle\hat{p}\rangle\rangle$. For the specific measurement

run shown in Fig. 2a, $|\alpha\rangle \approx |3 + 3i\rangle$. Figure 2b illustrates the measurements at the homodyne detector HD1 after the four-mode state has been transmitted through the channel with erasure on channel 2. The state is clearly seen to be corrupted as the first and second moments of the quantum oscillator are significantly changed. However, by using the measurement outcomes (x_m, p_m) of the homodyne detectors (Fig. 2c) to linearly displace the amplitude and phase quadratures of the transmitted state (x_o, p_o) with the gain, G ($x_o \rightarrow x_o + \sqrt{G}x_m, p_o \rightarrow p_o + \sqrt{G}p_m$), the original quantum state is partially recovered, as shown qualitatively in Fig. 2d for $G = 1.97$. The accuracy in the estimation of the error (and thus the precision of the displacement) depends crucially on the degree of squeezing: by using infinite squeezing, the transmitted states can, in principle, be perfectly corrected¹⁵. With finite squeezing the protocol can be quantified by the fidelity between the input state and the corrected output state. Based on the measurements presented above, the fidelities are computed for various gains and the results are depicted by the blue squares in Fig. 2e. A maximum fidelity of 0.57 ± 0.02 is obtained, which clearly surpasses the classical benchmark of 0.50. Similar fidelities are achieved for the erasure of channel 1, whereas fidelities close to unity are obtained when channels 3 or 4 are blocked. Measurements for which the two-mode squeezed state was replaced by vacua were also carried out for different displacement gains. The resulting fidelities are depicted in Fig. 2e by the red circles, and they nicely illustrate the need for entanglement. Although the protocol has been implemented only for a specific pair of input coherent states, it will work equally well for any coherent state as the protocol is invariant under displacements. Thus any input alphabet of coherent states can be corrected.

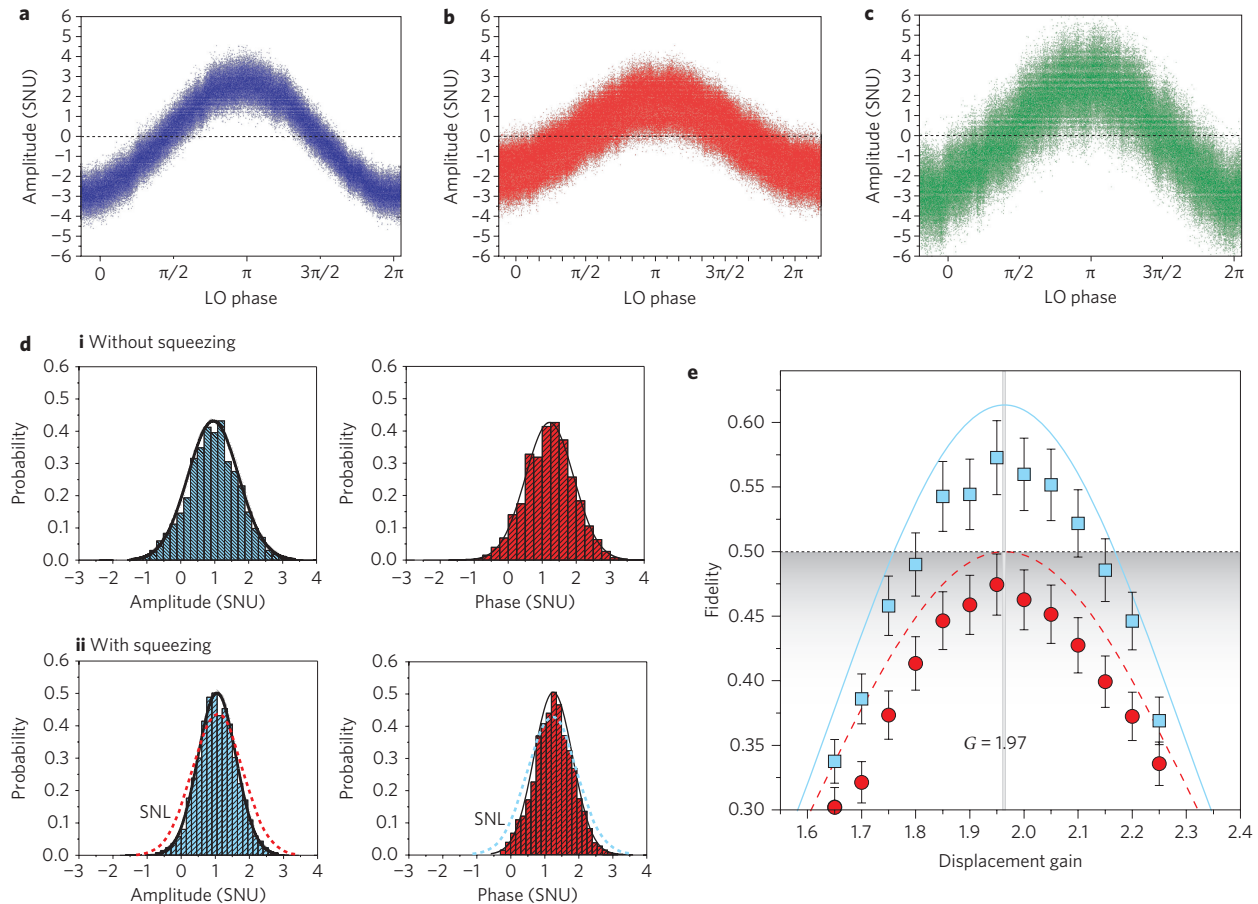


Figure 2 | Results of the deterministic QECC protocol. **a**, Phase scan of the input coherent state with the excitation $|\alpha\rangle \approx |3 + 3i\rangle$. **b,c**, Phase scans of the output state measured at HD1 before correction (**b**) and of the corrected output state (**c**). **d**, Histograms of the marginal distributions of the amplitude and phase quadratures of the joint syndrome measurement (in shot noise units, SNU). Red and blue curves correspond to the marginal distributions for a shot-noise-limited (SNL) state, whereas the black curves are the best Gaussian fits to the histograms. **e**, Fidelity is plotted as a function of the displacement gain with (blue squares) and without (red circles) the use of entanglement. The dashed and solid lines are the theoretically predicted fidelities for 0 dB and 2 dB of two-mode squeezing, respectively. The error bars depend on the measurement error, which is mainly associated with the stability of the system over time and the finite resolution of the analog-to-digital converter. This amounts to an error of $\pm 3\%$ for all fidelities.

We now proceed by discussing the results of probabilistic recovery of quantum information, where the objective is to use a probabilistic QECC to surpass the fidelity associated with a single channel. In contrast to the deterministic approach, for which stringent conditions are put on the channels, the probabilistic approach is much less stringent. One may allow for multiple erasures and, in addition, there are no requirements regarding knowledge of the occurrence and location of the erasures. In this case, the density matrix of the transmitted state is given by

$$\rho_{\text{trans}} = \sum_{i=1}^{16} P_i \rho_i \quad (2)$$

where ρ_i is the output density matrix corresponding to one of the 16 different erasure patterns that may occur during transmission and P_i indicates the associated probability running from P_E^4 to $(1 - P_E)^4$ corresponding to complete erasure and complete transmission, respectively. Using the tomographic maximum likelihood algorithm for reconstructing the density matrices via homodyne detection, we fully characterized the input and output states for various cases. Figure 3a shows the density matrix of the coherent input state in the 30×30 Fock state basis. This state was then mixed with the entangled state and sent through the four channels.

Subsequently, we performed 16 different full measurement runs by interchangeably blocking the four channels corresponding to the 16 different transmission patterns. The measurement outcomes are then weighted by the probabilities P_i to create the density matrix of the transmitted mixed state. The corrupted states were then probabilistically corrected by conditioning on the outcomes of the syndrome measurements (SMs). For the realization in Fig. 3 we used the condition that if the measurement outcomes obeyed $|x_m| > 0.8$ and $|p_m| > 0.8$ (found from optimization¹⁵), an error was detected and the resulting transmitted state was discarded. After this filtering operation, we reconstructed the density matrix based on the reduced data set; the result is shown in Fig. 3c for $P_E = 0.25$. By replacing the entangled states with vacua, the resulting density matrix is largely changed, as illustrated in Fig. 3d. To determine the fidelity F between the input state (with density matrix ρ_{in}) and the filtered output state (with density matrix ρ_{out}), we used the general expression $F = [\text{Tr}(\sqrt{\sqrt{\rho_{\text{out}}}\rho_{\text{in}}\sqrt{\rho_{\text{out}}}})]^2$. For the example in Fig. 3c we computed a fidelity of $F = 0.82 \pm 0.02$, which clearly surpasses the transmission fidelity of $F \simeq 0.75$ obtained by transmission in a single channel with similar erasure probability and with no error correction applied. It is interesting to note that even without entanglement, the protocol also outperforms the single channel approach¹⁵. For the corresponding entanglement-free set-up, in which the two-mode squeezed state is replaced by vacua, the corrected density

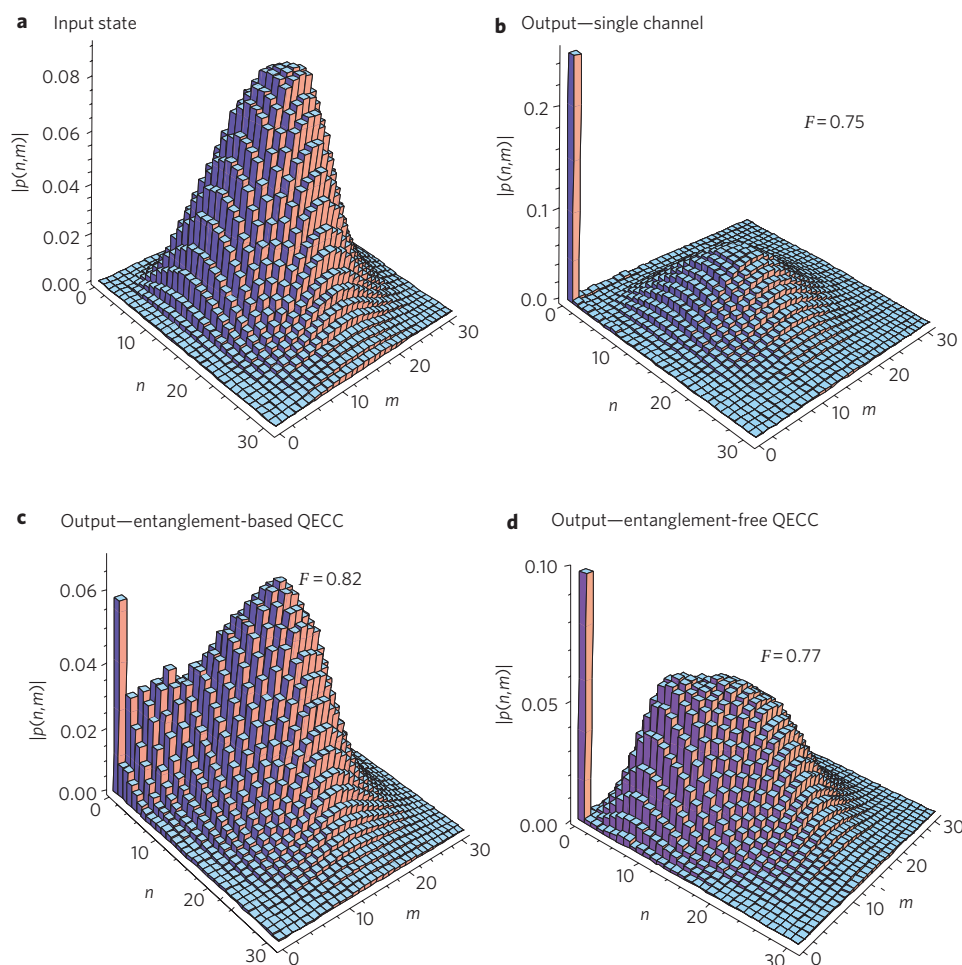


Figure 3 | Results of the probabilistic QECC protocol. **a**, Density matrix in the 30×30 Fock state basis of the input coherent state with the excitation $|\alpha\rangle \approx |3 + 3\rangle$. **b**, Density matrix of the output state using a single erasure channel as described in equation (1). The fidelity to the input state is $F = 0.75$. **c**, Density matrix of the corrected output state using the entangled four-mode code. The fidelity to the input state is $F = 0.82$. **d**, Density matrix for the corrected output state when the entangled states are blocked, and thus replaced by vacua. The fidelity is computed to be $F = 0.77$. The erasure probability for all realizations is $P_E = 0.25$.

matrix is shown in Fig. 3c and a fidelity of $F = 0.77 \pm 0.02$ is computed.

The fidelity as a function of the error probability P_E and the threshold value $|x_{th}| = |p_{th}|$ are illustrated in Fig. 4a and b, respectively. It can be seen that the entanglement-free QECC performs better than the single channel approach (that is, without error correction) for error probabilities up to $\sim 28\%$. It is also evident that the use of the entanglement-based code further increases the fidelity for all evaluated error probabilities. As expected, we see in Fig. 4b that the fidelity increases as the threshold value is lowered. This is associated, however, with a lower probability of success.

We have successfully demonstrated a continuous-variable quantum erasure-correcting code that protects quantum optical coherence from erasures (or probabilistic photon losses). The deterministic version of our scheme has the additional advantage that it enables a direct processing of the error-corrected output state in downstream applications, circumventing the need for a quantum repeater configuration that requires quantum entanglement distillation and quantum memory. Moreover, the deterministic version may be relevant in the perspective of fault-tolerant implementation of CV quantum information computing: probabilistic gates are applied at the level of the encoded states and gate success (or failure) translates into transmission (or erasure) of the corresponding mode.

Although the protocol has only been experimentally accessed for quantum information encoded in coherent states of light, it enables the faithful transmission of other quantum states such as squeezed states, qubit states or even bipartite entangled states. Furthermore, the error model can be extended to also include partial erasure and random phase noise, which often occurs in free-space transmission in a turbulent atmosphere²¹. As an outlook, it is intriguing to address the universality of our protocol with respect to arbitrary input states and arbitrary non-Gaussian error models.

Methods

Generation of two-mode squeezing. Two-mode squeezing (or CV entanglement) was produced through the interference of two single-mode squeezed states generated in optical parametric oscillators (OPOs) operating below threshold. The main source for the OPOs was a Diabolo laser (Innolight) delivering 400 mW of infrared light (1,064 nm) and 600 mW of green light (532 nm). These light beams were both sent through empty, high-finesse triangular cavities to clean their spatial modes as well as to filter out classical amplitude and phase noise. The resulting beams then served as pump beams, seed beams and locking beams for the OPOs. The OPOs were bow-tie-shaped cavities each with a type I periodically poled potassium titanyl phosphate (KTP) crystal ($1 \times 2 \times 10 \text{ mm}^3$) for nonlinear downconversion. The OPO cavities each consisted of two curved mirrors (radius of curvature, 25 mm) and two plane mirrors. Three of the mirrors in each cavity were highly reflective at 1,064 nm ($R > 99.95\%$), and the output couplers had a transmission of 8%. The transmittance of the mirrors at the pump wavelength (532 nm) was more than 95%. Together with

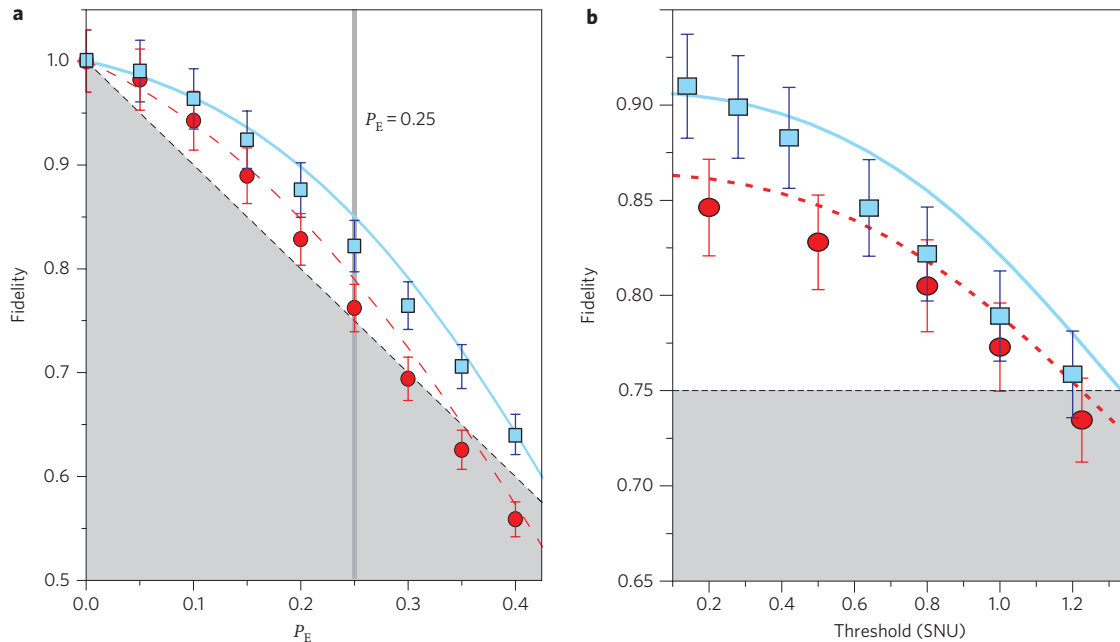


Figure 4 | Performance of the probabilistic QECC protocol. a,b, Transmission fidelity plotted as a function of the erasure probability (**a**) and the post-selection threshold value (**b**). In both plots the dashed line represents the single channel (code-free) fidelity. The circles correspond to the entanglement-free error correction code, and the squares correspond to the entanglement-based code. The dashed and solid lines are the theoretically predicted fidelities for the two cases. The directly measured squeezing values at the entrance to the protocol were ~ 3 dB (see Methods). The black dotted lines are the fidelity for the transmission in a single channel. For the theoretical model, we used a single-mode picture¹⁵ which is justified by the small bandwidth of the measurements (300 kHz); otherwise a broadband description should be used²⁶. The error bars are estimated as explained in the caption of Fig. 2.

the pump, a seed beam was injected at 1,064 nm, the brightness of which facilitated the construction of the various phase locks in the set-up. To lock the phase of the cavities we used auxiliary counterpropagating beams at 1,064 nm. Amplitude quadrature squeezed beams were then produced by deamplification of the seed beams. Using a spectrum analyser we measured squeezing of -3.4 ± 0.2 dB and -2.7 ± 0.2 dB below the shot noise level (at 5.5 MHz, a resolution bandwidth of 300 kHz and video bandwidth of 300 Hz) for the two OPOs. The two amplitude squeezed beams with a relative phase of $\pi/2$ were then brought to interference at a 50/50 beamsplitter (visibility greater than 98%) to produce the two-mode squeezing, which was then launched into the quantum error correction coding set-up. The average measured two-mode squeezing was approximately -2.0 ± 0.5 dB below the shot noise level.

Data acquisition. All measurements were performed at a sideband frequency of 5.5 MHz. The electronic outputs of all detectors were mixed down with an electronic local oscillator at 5.5 MHz, low-pass filtered (300 kHz), amplified (FEMTO DHPVA-100) and finally digitized by a 14-bit analog-to-digital converter at 10 Msamples/s. The signal was sampled around the 5.5 MHz sideband to avoid low-frequency classical noise. The time trace of the coherent state is shown in Fig. 2 before (Fig. 2a) and after (Fig. 2b) total erasure of channel 2 (see Fig. 1). These are typical traces of a homodyne measurement of a coherent state, where the local oscillator is scanned from 0 to 2π . The traces consist of $\sim 220,000$ data points. From the down-mixed time traces we reconstructed the density matrices and the Wigner functions using a maximum likelihood algorithm.

Received 10 March 2010; accepted 10 June 2010;
published online 25 July 2010

References

- Nielsen, M. A. & Chuang, I. L. *Quantum Computation and Quantum Information* (Cambridge Univ. Press, 2000).
- Shor, P. W. Scheme for reducing decoherence in quantum computer memory. *Phys. Rev. A* **52**, R2493–R2496 (1995).
- Steane, A. M. Error correcting codes in quantum theory. *Phys. Rev. Lett.* **77**, 793–797 (1996).
- Calderbank, A. R. & Shor, P. W. Good quantum error-correcting codes exist. *Phys. Rev. A* **54**, 1098–1105 (1996).
- Laflamme, R., Miquel, C., Paz, J. P. & Zurek, W. H. Perfect quantum error correcting code. *Phys. Rev. Lett.* **77**, 198–201 (1996).
- Bennett, C. H., DiVincenzo, D. P., Smolin, J. A. & Wootters, W. K. Mixed-state entanglement and quantum error correction. *Phys. Rev. A* **54**, 3824–3851 (1996).
- Grassl, M., Beth, Th. & Pellizzari, T. Codes for the quantum erasure channel. *Phys. Rev. A* **56**, 33–38 (1997).
- Braunstein, S. Error correction for continuous quantum variables. *Phys. Rev. Lett.* **80**, 4084–4087 (1998).
- Lloyd, S. & Slotine, J.-J. E. Analog quantum error correction. *Phys. Rev. Lett.* **80**, 4088–4091 (1998).
- Braunstein, S. L. Quantum error correction for communication with linear optics. *Nature* **394**, 47–49 (1998).
- Duan, L. M., Lukin, M. D., Cirac, J. I. & Zoller, P. Long-distance quantum communication with atomic ensembles and linear optics. *Nature* **414**, 413–418 (2001).
- Yuan, Z.-S. *et al.* Experimental demonstration of a BDCZ quantum repeater node. *Nature* **454**, 1098–1101 (2008).
- Knill, E. Quantum computing with realistically noisy devices. *Nature* **434**, 39–44 (2005).
- Wilde, M. M., Krovi, H. & Brun, T. A. Entanglement-assisted quantum error correction with linear optics. *Phys. Rev. A* **76**, 052308 (2007).
- Niset, J., Andersen, U. L. & Cerf, N. J. Experimentally feasible quantum erasure-correcting code for continuous variables. *Phys. Rev. Lett.* **101**, 130503 (2008).
- Cory, D. G. *et al.* Experimental quantum error correction. *Phys. Rev. Lett.* **81**, 2152–2155 (1998).
- Chiaverini, J. *et al.* Realization of quantum error correction. *Nature* **432**, 602–605 (2004).
- Pittmann, T. B., Jacobs, B. C. & Franson, J. D. Demonstration of quantum error correction using linear optics. *Phys. Rev. A* **71**, 052332 (2005).
- Aoki, T. *et al.* Quantum error correction beyond qubits. *Nature Phys.* **5**, 541–546 (2009).
- Wittmann, C. *et al.* Quantum filtering of optical coherent states. *Phys. Rev. A* **78**, 032315 (2008).
- Majumdar, A. K. & Ricklin, J. C. *Free-Space Laser Communications* (Springer, 2008).
- Elser, D. *et al.* Feasibility of free space quantum key distribution with coherent polarization states. *N. J. Phys.* **11**, 045014 (2009).
- Niset, J., Fiurasek, J. & Cerf, N. J. No-go theorem for Gaussian quantum error correction. *Phys. Rev. Lett.* **102**, 120501 (2009).
- Lance, A. M. *et al.* Tripartite quantum state sharing. *Phys. Rev. Lett.* **92**, 177903 (2004).
- Niset, J. *et al.* Superiority of entangled measurements over all local strategies for the estimation of product coherent states. *Phys. Rev. Lett.* **98**, 260404 (2007).
- Van Loock, P. *et al.* Broadband teleportation. *Phys. Rev. A* **62**, 022309 (2000).

Acknowledgements

This work was supported by the Future and Emerging Technologies programme of the European Commission under the FP7 FET-Open grant no. 212008 (COMPAS), by the Danish Agency for Science Technology and Innovation under grant no. 274-07-0509, by the Deutsche Forschungsgesellschaft, and by the Interuniversity Attraction Poles program of the Belgian Science Policy Office under grant IAP P6-10 (photonics@be).

Author contributions

M.L. and M.S. performed the experiments. J.N. and N.J.C. performed the theoretical calculations. M.L., M.S. and A.H. performed the data analysis. M.L., N.J.C. and U.L.A.

wrote the manuscript. M.L., M.S., U.L.A. and G.L. performed the project planing. All authors discussed the results and implications and commented on the manuscript at all stages. Correspondence and requests for additional materials should be addressed to M.L. or U.L.A.

Additional information

The authors declare no competing financial interests. Reprints and permission information is available online at <http://npg.nature.com/reprintsandpermissions/>. Correspondence and requests for materials should be addressed to M.L. and U.L.A.